Critical slope singularities in rotating and stratified fluids

Stéphane Le Dizès*
Aix Marseille Université, CNRS, Centrale Méditerranée, IRPHE, F-13013 Marseille, France

(Received 19 July 2023; accepted 27 February 2024; published 22 March 2024)

A rotating or stratified fluid supports waves that propagate in fixed directions. If the fluid is uniformly rotating around an axis Oz with a rotation rate Ω and/or uniformly stratified along the same axis with a Brunt-Väisälä frequency N, then harmonic waves of frequency ω propagate along characteristic lines that make an angle θ with respect to the horizontal plane Oxy with θ satisfying the relation $\omega^2 = 4\Omega^2 \cos^2\theta + N^2 \sin^2\theta$. Any infinitesimal oscillation of the boundary is a source of waves, but when this boundary is tangent to a direction of propagation of the waves, a singularity generically appears. This critical slope singularity propagates along the critical ray tangent to the boundary. When weak viscous effects are considered, this singular ray forms a concentrated self-similar wave beam with an amplitude that depends on the nature of the singularity and a width of order $(\nu x_\parallel/\omega)^{1/3}$, where ν is the kinematic viscosity and $x_\parallel$ the distance to the critical point measured along the beam. The goal of the present work is to provide information on the type of singularities that can be generated in an infinite domain and therefore on the amplitude and nature of the concentrated wave beams that can be created from critical points. We analyze in a two-dimensional framework two generic configurations corresponding to oscillations normal and tangent to the boundary, respectively. In the first case (oscillations normal to the boundary), we obtain an amplitude scaling in $[\omega r_c^3/(\nu x_\parallel)]^{1/6}$ corresponding to an inviscid singularity in $x_\perp^{-1/2}$, where $x_\perp$ is the distance to the critical ray and r_c the radius of curvature at the critical point. In the second case (oscillations tangent to the boundary), a weaker beam in $[\nu r_c^3/(\omega x_\parallel^5)]^{1/12}$ is obtained corresponding to a stronger singularity in $x_\perp^{-5/4}$. In that case, the beam is generated by the particular viscous boundary layer flow obtained close to the critical point and the problem can be completely solved by a local analysis. A general expression for the beam amplitude is derived that depends on the fluid characteristics (Ω, N), the wave frequency ω, the velocity amplitude of imposed tangential oscillations, and the local radius of curvature at the critical point. Finally, the first-order viscous correction to the critical slope beam induced by the no-slip boundary condition on the surface is also calculated.

DOI: 10.1103/PhysRevFluids.9.034803

I. INTRODUCTION

In a fluid rotating and uniformly stratified along a same axis Oz, inertia-gravity waves have the particularity of propagating along characteristic directions making an angle θ with respect to the horizontal plane that depends only on the ratio of the wave frequency with the background characteristic frequencies (Brunt-Väisälä frequency N and rotation rate Ω). When one of these directions of propagation is tangent to a surface which is potentially a source of waves, a singularity generically appears along this direction. This so-called critical slope singularity is the subject of the present paper.

*stephane.ledizes@univ-amu.fr

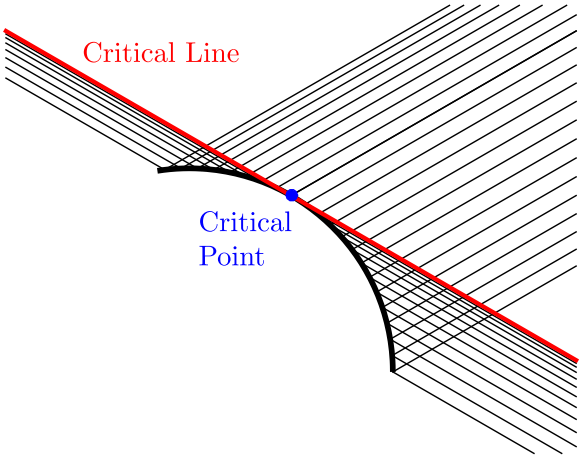

FIG. 1. Illustration of the ray accumulation on the critical line. Rays (thin black lines) are emitted from equidistant points on an arc of circle (thick black line) in the characteristic directions (here $\theta = -\pi/6$, $\pi/6, 5\pi/6$). The distance between consecutive rays is the smallest close to the critical line (red solid line) tangent to the surface at the critical point (blue circle).

Figure 1 illustrates the mechanism responsible of the singularity. It shows that if sources were equidistantly placed on the surface of an object, then the rays emitted from these sources will tend to accumulate along the characteristic line tangent to the object. The same phenomenon occurs when a plane wave is reflected by supercritical topography [1].

The footprint of this singularity is clearly visible in experiments. It corresponds to the Saint Andrews cross that is formed when a small object is oscillated at a frequency in the inertia-gravity wave frequency range [2,3]. The wave structure obtained from an oscillating cylinder or an oscillating sphere has been analyzed in several studies (see, for instance, Refs. [4–6]). The reader is referred to Voisin's work [7,8] for more references and a comprehensive discussion of the literature.

In the ocean, this singularity is expected to appear when the oscillating tide interacts with a supercritical topography, that is a topography which exhibits a critical slope. This interaction has been studied experimentally (see, for instance, Ref. [9]), theoretically [10], and numerically [11].

The structure of the concentrated wave beam associated with this singularity has been the subject of many works in both rotating fluids [12–15] and stratified fluids [16,17]. The self-similar expression introduced in Refs. [14,17] was shown to describe correctly both the far-field of a localized wave source [18,19], and the intense shear layer emitted from sharp edges [20] and critical slopes [13].

In the present work, we focus on the generic features of the critical slope singularities. Our goal is to provide informations on these singularities and show how they completely govern the structure and strength of the intense shear layers along the critical line.

The paper is organized as follows. In Sec. II, we first show how the outward radiation condition and the inviscid nonpenetration condition on the boundary close to a critical point provide informations on the amplitude and strength of the critical slope singularity. In Sec. III, we explain how the inviscid singularity is smoothed by viscosity. The amplitude and structure of the intense shear layer obtained along the critical line is thus given in this section. Two generic configurations corresponding to a normal and a tangential oscillation of the boundary are then analyzed in details in Sec. IV. The singularity generated by the tangential oscillation is due to the Ekman pumping in the viscous boundary layer. The calculation of the Ekman pumping close to a critical point is provided in Appendix. In Sec. V, we provide the first-order viscous correction to the solution derived in Sec. III. A brief discussion of the results and their possible extension is finally given in Sec. VI.

II. INVISCID ANALYSIS OF CRITICAL SLOPE SINGULARITIES

We consider a weakly viscous incompressible fluid, of kinematic viscosity ν, uniformly rotating around a vertical axis $\mathbf{e}_z$ (oriented upwards) at a constant rotation rate Ω, and uniformly stratified along the same axis with a constant Brunt-Väisälä frequency N. The buoyancy diffusivity is neglected and the reference density is fixed to unity.

We are interested in the properties of waves generated by small oscillations of a finite object in an infinite domain. The domain and all the fields are assumed to be independent of the spatial variable y so that the analysis can be performed in the (Oxz) plane.

The velocity $\mathbf{U}$, pressure P, and buoyancy B are assumed to be governed by the Navier-Stokes equations under the Boussinesq approximation,

$$\frac{D\mathbf{U}}{Dt} + 2\Omega\mathbf{e}_z \times \mathbf{U} = -\boldsymbol{\nabla} P + B\mathbf{e}_z + \nu\Delta\mathbf{U}, \tag{1a}$$

$$\frac{DB}{Dt} + N^2\mathbf{e}_z \cdot \mathbf{U} = 0, \tag{1b}$$

$$\boldsymbol{\nabla} \cdot \mathbf{U} = 0, \tag{1c}$$

where $D/Dt = \partial/\partial_t + \mathbf{U} \cdot \boldsymbol{\nabla}$.

We are interested in linear time-harmonic fluctuations that can be written as

$$(\mathbf{U}, P, B) = (\mathbf{u}, p, b)e^{-i\omega t} + \text{c.c.} \tag{2}$$

where c.c. denotes the complex conjugate. The amplitudes $\mathbf{u} = (u_x, u_y, u_z)$, p, and b satisfy the following system deduced from the linearization of (1a)–1(c):

$$-i\omega\mathbf{u} + 2\Omega\mathbf{e}_z \times \mathbf{u} = -\boldsymbol{\nabla} p + b\mathbf{e}_z + \nu\Delta\mathbf{u}, \tag{3a}$$

$$-i\omega b + N^2 w = 0, \tag{3b}$$

$$\boldsymbol{\nabla} \cdot \mathbf{u} = 0. \tag{3c}$$

Equation (3c) reads, for a velocity field independent of y, as $\partial_x u_x + \partial_z u_z = 0$. This allows us to introduce a stream function $\psi(x, z)$ for the 2D velocity field $\mathbf{u}_{2\mathrm{D}} = (u_x, u_z)$ such that $u_x = -\partial_z\psi$ and $u_z = \partial_x\psi$. In an inviscid framework ($\nu = 0$), this function is found to satisfy the Poincaré equation,

$$\left[-\omega^2\left(\frac{\partial^2}{\partial x^2} + \frac{\partial^2}{\partial z^2}\right) + 4\Omega^2\frac{\partial^2}{\partial z^2} + N^2\frac{\partial^2}{\partial x^2}\right]\psi = 0\,. \tag{4}$$

For a rotating fluid ($\Omega \neq 0$), the velocity component u_y along y is nonzero and given by

$$u_y = -\frac{2i\Omega}{\omega}u_x = \frac{2i\Omega}{\omega}\frac{\partial\psi}{\partial z}. \tag{5}$$

Similarly, for a stratified fluid ($N \neq 0$), there is a buoyancy perturbation given by

$$b = -\frac{iN^2}{\omega}u_z = -\frac{iN^2}{\omega}\frac{\partial\psi}{\partial x}. \tag{6}$$

We shall assume that the frequency ω is between N and 2Ω. In that case, Eq. (4) is a homogeneous hyperbolic equation whose characteristics are the lines that make an angle θ with respect to the horizontal plane given by

$$\omega^2 = 4\Omega^2\cos^2\theta + N^2\sin^2\theta. \tag{7}$$

We can assume that $0 \leqslant \theta \leqslant \pi/2$. The three other solutions of (7) are $-\theta$, $\pi + \theta$, and $\pi - \theta$.

We shall consider solutions above a 2D y-independent surface whose cross section in the plane (Oxz) will be defined by a curve $\mathcal{S}$. Only the three directions θ, $\pi - \theta$, and $-\theta$ will correspond to possible directions of propagation from the surface to the fluid domain. They will be denoted by NE (north-east), NW (north-west), and SE (south-east), respectively. It is useful to introduce several

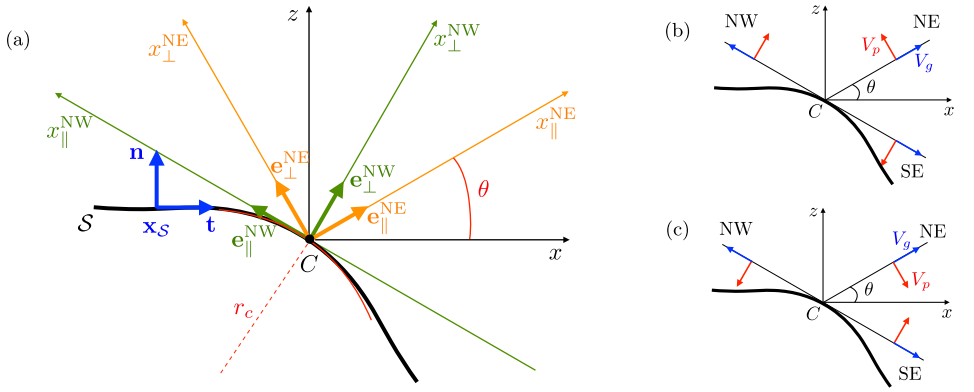

FIG. 2. (a) Coordinate systems near the critical point C. Two orthogonal bases $(\mathbf{e}_\parallel^{\mathrm{NW}}, \mathbf{e}_\perp^{\mathrm{NW}})$ and $(\mathbf{e}_\parallel^{\mathrm{NE}}, \mathbf{e}_\perp^{\mathrm{NE}})$ are introduced to characterize the solutions propagating along characteristic lines in the NW and NE directions, respectively. The vector $\mathbf{e}_\parallel^{\mathrm{NW}}$ is tangent to the boundary at the critical point and the line $x_\perp^{\mathrm{NW}} = 0$ defines the critical line. The orthogonal basis $(\mathbf{t}, \mathbf{n})$ is constructed using the local tangent and normal vector to the curve $\mathcal{S}$ at the point $\mathbf{x}_{\mathcal{S}}$. The radius of curvature of the curve $\mathcal{S}$ at C is r_c. [(b) and (c)] Relation between phase velocity and group velocity orientations in the different directions of propagation for (b) $N < 2\Omega$ and (c) $2\Omega < N$.

orthogonal vector bases associated with the boundary curve $\mathcal{S}$ and the directions of propagation. These different bases are sketched in Fig. 2(a) for a generic configuration close to a critical point C. The local Frenet basis $(\mathbf{t}, \mathbf{n})$ at the point $\mathbf{x}_{\mathcal{S}}$ on the curve $\mathcal{S}$ is defined such that the normal vector $\mathbf{n}$ is oriented towards the fluid domain. The bases $(\mathbf{e}_\parallel^{\mathrm{NW}}, \mathbf{e}_\perp^{\mathrm{NW}})$ and $(\mathbf{e}_\parallel^{\mathrm{NE}}, \mathbf{e}_\perp^{\mathrm{NE}})$ are associated with the solutions propagating in the NW and NE directions, respectively. We also define the coordinate systems $(x_\parallel^{\mathrm{NW}}, x_\perp^{\mathrm{NW}})$ and $(x_\parallel^{\mathrm{NE}}, x_\perp^{\mathrm{NE}})$ associated with these bases such that the origin in both frames is at the critical point C. Vectors and coordinates associated with the directions of propagation can be expressed in term of Cartesian quantities as

$$\mathbf{e}_\parallel^{\mathrm{NW}} = -\cos\theta\,\mathbf{e}_x + \sin\theta\,\mathbf{e}_z, \qquad \mathbf{e}_\perp^{\mathrm{NW}} = \sin\theta\,\mathbf{e}_x + \cos\theta\,\mathbf{e}_z, \tag{8a}$$

$$\mathbf{e}_\parallel^{\mathrm{NE}} = \cos\theta\,\mathbf{e}_x + \sin\theta\,\mathbf{e}_z, \qquad \mathbf{e}_\perp^{\mathrm{NE}} = -\sin\theta\,\mathbf{e}_x + \cos\theta\,\mathbf{e}_z, \tag{8b}$$

$$x_\parallel^{\mathrm{NW}} = -\cos\theta\,x + \sin\theta\,z, \qquad x_\perp^{\mathrm{NW}} = \sin\theta\,x + \cos\theta\,z, \tag{8c}$$

$$x_\parallel^{\mathrm{NE}} = \cos\theta\,x + \sin\theta\,z, \qquad x_\perp^{\mathrm{NE}} = -\sin\theta\,x + \cos\theta\,z. \tag{8d}$$

We have not introduced the local basis associated with SE direction. The solution propagating in that direction will be described using the basis $(\mathbf{e}_\parallel^{\mathrm{NW}}, \mathbf{e}_\perp^{\mathrm{NW}})$ and the variables $(x_\parallel^{\mathrm{NW}}, x_\perp^{\mathrm{NW}})$.

With these new variables, Eq. (4) can simply be written as

$$\frac{\partial}{\partial x_\perp^{\mathrm{NE}}}\frac{\partial}{\partial x_\perp^{\mathrm{NW}}}\psi = 0, \tag{9}$$

so its general solution can be written as

$$\psi(x,z) = F(x_\perp^{\mathrm{NE}}) + G(x_\perp^{\mathrm{NW}}), \tag{10}$$

where F and G are two arbitrary functions. The velocity field $\mathbf{u}_{2\mathrm{D}}$ [in the (x,z) plane] becomes

$$\mathbf{u}_{2\mathrm{D}} = -F'(x_\perp^{\mathrm{NE}})\mathbf{e}_\parallel^{\mathrm{NE}} + G'(x_\perp^{\mathrm{NW}})\mathbf{e}_\parallel^{\mathrm{NW}}. \tag{11}$$

In general, G describes waves propagating in both $\mathbf{e}_\parallel^{\mathrm{NW}}$ and $\mathbf{e}_\parallel^{\mathrm{SE}} = -\mathbf{e}_\parallel^{\mathrm{NW}}$. The part that is propagating in a given direction is obtained by splitting the Fourier decomposition of G into positive

and negative wave numbers

$$G(x_\perp^{\mathrm{NW}}) = \int_0^{+\infty} \hat{G}(k) e^{ikx_\perp^{\mathrm{NW}}} dk + \int_{-\infty}^{0} \hat{G}(k) e^{ikx_\perp^{\mathrm{NW}}} dk. \tag{12}$$

The first part, associated with positive k, describes a wave packet with phase velocities oriented along $\mathbf{e}_\perp^{\mathrm{NW}}$ (assuming $\omega > 0$). The group velocity of this wave packet, that gives the direction of propagation, is oriented along $\mathbf{e}_\parallel^{\mathrm{NW}}$ if $N < 2\Omega$ but along $-\mathbf{e}_\parallel^{\mathrm{NW}}$ if $N > 2\Omega$ [see Figs. 2(b) and 2(c)]. This means that if $N < 2\Omega$, then the wave packet composed of positive wave numbers propagates in the direction of $\mathbf{e}_\parallel^{\mathrm{NE}}$ and the one with negative wave numbers propagates in the direction $-\mathbf{e}_\parallel^{\mathrm{NW}}$. The opposite holds if $N > 2\Omega$.

As explained by Baines [21], the condition of causality can be directly expressed as a condition on the functions F and G. For instance, the function G defines a wave packet that propagates in the NW direction if

$$G(x_\perp^{\mathrm{NW}}) = -\frac{i\epsilon}{\pi} P \int_{-\infty}^{\infty} \frac{G(\eta)}{\eta - x_\perp^{\mathrm{NW}}} d\eta\,, \tag{13}$$

where the P in front of the integral means that the Cauchy principal part of the integral is taken. The wave packet propagating in the SE direction satisfies

$$G(x_\perp^{\mathrm{NW}}) = \frac{i\epsilon}{\pi} P \int_{-\infty}^{\infty} \frac{G(\eta)}{\eta - x_\perp^{\mathrm{NW}}} d\eta\,. \tag{14}$$

In these equations, $\epsilon = \mathrm{sgn}(2\Omega - N)$. When $\epsilon = -1$, we recover the conditions obtained by Baines [21] for the nonrotating case. As we are going to see, these equations are useful to implement the outward boundary condition on the solutions emitted from the neighborhood of the critical point.

Let us now consider the constraints that we obtain on the solution by applying the boundary conditions close to the critical point C. We assume that the waves are generated by the displacement of the boundaries. In an inviscid framework, at any point $\mathbf{x}_\mathcal{S}$ of the boundary $\mathcal{S}$, the velocity field amplitude $\mathbf{u}$ should satisfy the no-penetration condition,

$$\mathbf{u}(\mathbf{x}_\mathcal{S}) \cdot \mathbf{n}(\mathbf{x}_\mathcal{S}) = \mathbf{u}_{2\mathrm{D}}(\mathbf{x}_\mathcal{S}) \cdot \mathbf{n}(\mathbf{x}_\mathcal{S}) = U_{0n}(\mathbf{x}_\mathcal{S}), \tag{15}$$

where $U_{0n}(\mathbf{x}_\mathcal{S})$ and $\mathbf{n}(\mathbf{x}_\mathcal{S})$ are the normal velocity amplitude and normal vector of the boundary at $\mathbf{x}_\mathcal{S}$.

As explained above, the geometry of the problem close to the critical point can generically be sketched as shown in Fig. 2(a). The origin of the different coordinate systems has been chosen at the critical point. The critical line, tangent to the surface at the origin is given by the equation $x_\perp^{\mathrm{NW}} = 0$. The line $x_\perp^{\mathrm{NE}} = 0$ divides the domain into two regions.

We are looking for solutions close to the critical point. Close to that point, the equation of the curve $\mathcal{S}$ has a simple generic expression when it is expressed in terms of the variables $x_\perp^{\mathrm{NE}}$ and $x_\perp^{\mathrm{NW}}$,

$$x_\perp^{\mathrm{NW}} \underset{x_\perp^{\mathrm{NE}} \to 0}{\sim} -\frac{(x_\perp^{\mathrm{NE}})^2}{2r_c(\sin 2\theta)^2} \quad \text{for} \quad x_\perp^{\mathrm{NW}} < 0 \tag{16}$$

or

$$x_\perp^{\mathrm{NE}} \underset{x_\perp^{\mathrm{NW}} \to 0}{\sim} \begin{cases} \sqrt{2r_c|x_\perp^{\mathrm{NW}}|}\sin 2\theta & \text{for } x_\perp^{\mathrm{NE}} > 0, \quad x_\perp^{\mathrm{NW}} < 0 \\ -\sqrt{2r_c|x_\perp^{\mathrm{NW}}|}\sin 2\theta & \text{for } x_\perp^{\mathrm{NE}} < 0, \quad x_\perp^{\mathrm{NW}} < 0 \end{cases}, \tag{17}$$

where r_c is the radius of curvature at the critical point. Note that these equations only depend on the angle θ and on r_c. They break down when $\sin 2\theta = 0$, that is, $\theta = 0$ and $\theta = \pi/2$, which corresponds to the situation where the vectors $\mathbf{e}_\parallel^{\mathrm{NW}}$ and $\mathbf{e}_\parallel^{\mathrm{NE}}$ are parallel.

Close to the critical point, we can also express the Cartesian components of $\mathbf{n}(\mathbf{x}_\mathcal{S})$ in terms of $x_\perp^{\mathrm{NE}}$,

$$n_x(\mathbf{x}_\mathcal{S}) \underset{x_\perp^{\mathrm{NE}}\to 0}{\sim} \sin\theta - \frac{x_\perp^{\mathrm{NE}}}{2r_c\sin\theta}, \quad n_z(\mathbf{x}_\mathcal{S}) \underset{x_\perp^{\mathrm{NE}}\to 0}{\sim} \cos\theta + \frac{x_\perp^{\mathrm{NE}}}{2r_c\cos\theta}. \tag{18}$$

Using (11) for $\mathbf{u}_{2\mathrm{D}}$ and the expressions (8a) and (8b) for $\mathbf{e}_\parallel^{\mathrm{NW}}$ and $\mathbf{e}_\parallel^{\mathrm{NE}}$, $\mathbf{u}_{2\mathrm{D}}\cdot\mathbf{n}$ can then be written close to the critical point as

$$\mathbf{u}_{2\mathrm{D}}(\mathbf{x}_\mathcal{S})\cdot\mathbf{n}(\mathbf{x}_\mathcal{S}) \sim -\sin 2\theta\, F'(x_\perp^{\mathrm{NE}}) + \frac{x_\perp^{\mathrm{NE}}}{r_c\sin 2\theta}\, G'(x_\perp^{\mathrm{NW}}). \tag{19}$$

As the relation between $x_\perp^{\mathrm{NE}}$ and $x_\perp^{\mathrm{NW}}$ depends on the sign of $x_\perp^{\mathrm{NE}}$, we expect two expressions for ψ and $\mathbf{u}_{2\mathrm{D}}$,

$$\psi_+ = F(x_\perp^{\mathrm{NE}}) + G_+(x_\perp^{\mathrm{NW}}), \quad \mathbf{u}_{2D+} = -F'(x_\perp^{\mathrm{NE}})\mathbf{e}_\parallel^{\mathrm{NE}} + G'_+(x_\perp^{\mathrm{NW}})\mathbf{e}_\parallel^{\mathrm{NW}}, \quad \text{for} \quad x_\perp^{\mathrm{NE}} > 0, \tag{20a}$$

$$\psi_- = F(x_\perp^{\mathrm{NE}}) + G_-(x_\perp^{\mathrm{NW}}), \quad \mathbf{u}_{2D-} = -F'(x_\perp^{\mathrm{NE}})\mathbf{e}_\parallel^{\mathrm{NE}} + G'_+(x_\perp^{\mathrm{NW}})\mathbf{e}_\parallel^{\mathrm{NW}}, \quad \text{for} \quad x_\perp^{\mathrm{NE}} < 0. \tag{20b}$$

Note that only the function $G(x_\perp^{\mathrm{NW}})$ describing the propagation in the NW and SE directions need two expressions for $x_\perp^{\mathrm{NW}} < 0$ because we have two different boundary conditions (17) for the same $x_\perp^{\mathrm{NW}} < 0$ according to the sign of $x_\perp^{\mathrm{NE}}$. By contrast, a single function $F(x_\perp^{\mathrm{NE}})$ can be used as the boundary conditions are on two different intervals of $x_\perp^{\mathrm{NE}}$.

The condition (15) implies that close to the critical point for $x_\perp^{\mathrm{NW}} < 0$

$$-\sin 2\theta F'(x_\perp^{\mathrm{NE}}) + \sqrt{\frac{2|x_\perp^{\mathrm{NW}}|}{r_c}}G'_+(x_\perp^{\mathrm{NW}}) \sim U_{0n}(\mathbf{x}_\mathcal{S})$$

$$\text{with } x_\perp^{\mathrm{NE}} \sim \sqrt{2r_c|x_\perp^{\mathrm{NW}}|}\sin 2\theta, \quad \text{when} \quad x_\perp^{\mathrm{NE}} > 0, \tag{21a}$$

$$-\sin 2\theta F'(x_\perp^{\mathrm{NE}}) - \sqrt{\frac{2|x_\perp^{\mathrm{NW}}|}{r_c}}G'_-(x_\perp^{\mathrm{NW}}) \sim U_{0n}(\mathbf{x}_\mathcal{S})$$

$$\text{with } x_\perp^{\mathrm{NE}} \sim -\sqrt{2r_c|x_\perp^{\mathrm{NW}}|}\sin 2\theta, \quad \text{when} \quad x_\perp^{\mathrm{NE}} < 0. \tag{21b}$$

The function F defines a wave packet propagating in the north-east direction. This condition is written as

$$F'(x_\perp^{\mathrm{NE}}) = -\epsilon\frac{i}{\pi}P\int_{-\infty}^{\infty}\frac{F'(\eta)}{\eta - x_\perp^{\mathrm{NE}}}d\eta, \tag{22}$$

where $\epsilon = \mathrm{sgn}(2\Omega - N)$.

Similarly, the function G_+ and the function G_- define wave packets propagating in the north-west direction and in the south-east direction, respectively. The function G_+ must then satisfy (13) while G_- must satisfy (14)

$$G'_+(x_\perp^{\mathrm{NW}}) = -\epsilon\frac{i}{\pi}P\int_{-\infty}^{\infty}\frac{G'_+(\eta)}{\eta - x_\perp^{\mathrm{NW}}}d\eta, \tag{23a}$$

$$G'_-(x_\perp^{\mathrm{NW}}) = \epsilon\frac{i}{\pi}P\int_{-\infty}^{\infty}\frac{G'_-(\eta)}{\eta - x_\perp^{\mathrm{NW}}}d\eta. \tag{23b}$$

Moreover, for $x_\perp^{\mathrm{NW}} > 0$, there is a single domain, so G_+ and G_- define the same function

$$G_+(x_\perp^{\mathrm{NW}}) = G_-(x_\perp^{\mathrm{NW}}) \quad \text{for} \quad x_\perp^{\mathrm{NW}} > 0. \tag{24}$$

Equations (21a), (21b), (22), (23a), (23b), and (24) are the constraints obtained from the boundary conditions on the surface close to the critical point and at infinity for the 2D velocity field defined by (11). We can now look at what they imply for singular fields.

Assume for instance that the forcing normal velocity $U_{0n}(\mathbf{x}_S)$ behaves close to the critical point as

$$U_{0n}(\mathbf{x}_S) \underset{x_\perp^{\rm NE}\to 0}{\sim} \begin{cases} \dfrac{C_+}{(x_\perp^{\rm NE})^\beta} & \text{for } x_\perp^{\rm NE} > 0, \\ \dfrac{C_-}{(-x_\perp^{\rm NE})^\beta} & \text{for } x_\perp^{\rm NE} < 0. \end{cases} \tag{25}$$

The boundary conditions (21a) and (21b) indicate that $F'(x_\perp^{\rm NE})$ and $G'_\pm(x_\perp^{\rm NW})$ should behave for small values of their argument as

$$F'(x_\perp^{\rm NE}) \underset{x_\perp^{\rm NE}\to 0}{\sim} \begin{cases} \dfrac{D_+}{(x_\perp^{\rm NE})^\beta} & \text{for } x_\perp^{\rm NE} > 0, \\ \dfrac{D_-}{(-x_\perp^{\rm NE})^\beta} & \text{for } x_\perp^{\rm NE} < 0, \end{cases} \tag{26}$$

and

$$G'_+(x_\perp^{\rm NW}) \underset{x_\perp^{\rm NW}\to 0}{\sim} \frac{E_+}{(-x_\perp^{\rm NW})^{(\beta+1)/2}} \quad \text{for } x_\perp^{\rm NW} < 0, \tag{27a}$$

$$G'_-(x_\perp^{\rm NW}) \underset{x_\perp^{\rm NW}\to 0}{\sim} \frac{E_-}{(-x_\perp^{\rm NW})^{(\beta+1)/2}} \quad \text{for } x_\perp^{\rm NW} < 0. \tag{27b}$$

We also expect for $x_\perp^{\rm NW} > 0$ a behavior of $G_+ = G_- = G$ of the same nature

$$G'(x_\perp^{\rm NW}) \underset{x_\perp^{\rm NW}\to 0}{\sim} \frac{E_o}{(x_\perp^{\rm NW})^{(\beta+1)/2}} \quad \text{for } x_\perp^{\rm NW} > 0\,. \tag{28}$$

Equations (26), (27a), (27b), and (28) define the velocity field $\mathbf{u}_{2D}$ close to the lines $x_\perp^{\rm NW} = 0$ and $x_\perp^{\rm NE} = 0$. The other components u_y and b are obtained using (5) and (6). The velocity field $\mathbf{u}_{2D}$ depends on five coefficients D_-, D_+, E_-, E_+, and E_o. The relations between these coefficients are obtained by applying the constraints derived above from the boundary conditions.

Let us first consider the radiation condition (22) for F'. If F' exhibits the singular behavior (26) with a β satisfying $0 < \beta$, then the integral on the right-hand side of (22) is expected to be dominated by the contribution coming from the neighborhood of $x_\perp^{\rm NE} = 0$. The function F' in this integral can be replaced by its singular expression (26) if β also satisfies $\beta < 1$ so that the integral remains finite. If we do this replacement and use the following equalities:

$$\frac{i}{\pi} P \int_0^\infty \frac{d\eta}{(\eta - x)\eta^\beta} = \begin{cases} \dfrac{i\cos(\pi\beta)}{\sin(\pi\beta)x^\beta} & x > 0 \\ \dfrac{i}{\sin(\pi\beta)(-x)^\beta} & x < 0 \end{cases}, \tag{29a}$$

$$\frac{i}{\pi} P \int_{-\infty}^0 \frac{d\eta}{(\eta - x)(-\eta)^\beta} = \begin{cases} -\dfrac{i}{\sin(\pi\beta)x^\beta} & x > 0 \\ -\dfrac{i\cos(\pi\beta)}{\sin(\pi\beta)(-x)^\beta} & x < 0 \end{cases}, \tag{29b}$$

valid for $0 < \beta < 1$, then we obtain a relation between D^+ and D^-,

$$D^+ = e^{i\pi\beta\epsilon} D^-\,. \tag{30}$$

This relation is *a priori* valid for $0 < \beta < 1$. If $\beta \leqslant 0$, then $F'(x_\perp^{\mathrm{NE}})$ vanishes or is finite at $x_\perp^{\mathrm{NW}} = 0$. In that case, an estimate of the integral on the right-hand side of (22) cannot be obtained using the local behavior of F' close to 0. However, if β is not a negative integer, then one just has to differentiate F' once or several times so that its derivative satisfies (26) with a value of β between 0 and 1. Similarly, if $\beta > 1$, then the integral on the right-hand side of (22) does not converge, so this equation cannot be used. However, as above, if β is not a positive integer, then one can integrate F' once (or several times) so that the primitive of F' is less singular, and satisfies (26) with $0 < \beta < 1$. In both cases, one can then use the relation (30) for the coefficients of either derivatives or primitives of F'. Since differentiation and integration just change β by an integer, (30) is thus valid for any β provided β is not an integer. Finally, note that if $\beta = 0$, then (30) would prescribe no jump, that is no singularity.

The above relation obtained between D^+ and D^- demonstrates that the outward boundary condition induces a strong constraint on a singular solution. It implies that if the singular behavior is known on one side of the singularity, then the solution on the other side is immediately known: It has a similar singular behavior with the same singularity index and a phase-shifted amplitude.

The same analysis can be applied to the radiation conditions for G'_+ and G'_-. It leads to two other relations among E_o, E_+, and E_-,

$$E_o = i\epsilon e^{i\epsilon\pi\beta/2} E_+, \tag{31a}$$

$$E_o = -i\epsilon e^{-i\epsilon\pi\beta/2} E_-, \tag{31b}$$

provided that $(\beta + 1)/2$ is not an integer. These two equations also imply that

$$E_+ = -e^{-i\epsilon\pi\beta} E_- . \tag{32}$$

The last relations between the coefficients are obtained by applying the boundary conditions (21a) and (21b) on the surface,

$$-\sin 2\theta\, D_+ + \sqrt{\frac{2}{r_c}} (\sqrt{2r_c} \sin 2\theta)^\beta E_+ = C_+, \tag{33a}$$

$$-\sin 2\theta\, D_- - \sqrt{\frac{2}{r_c}} (\sqrt{2r_c} \sin 2\theta)^\beta E_- = C_-. \tag{33b}$$

Equations (30), (31a), (31b), (33a), and (33b) define a linear inhomogeneous system of five equations for the five unknown coefficients E_+, E_-, E_o, D_+, and D_-. It admits a unique solution whatever C_+ and C_- if and only if

$$e^{2i\pi\beta} \neq 1, \tag{34}$$

that is β is not an integer. This condition was already required to derive Eq. (30).

In that case, the unique solution is given by

$$D_+ = \epsilon \frac{C_- - e^{i\epsilon\pi\beta} C_+}{2i \sin\pi\beta\, \sin 2\theta}, \tag{35a}$$

$$D_- = \epsilon \frac{e^{-i\epsilon\pi\beta} C_- - C_+}{2i \sin\pi\beta\, \sin 2\theta}, \tag{35b}$$

$$E_+ = \epsilon \frac{C_- - e^{-i\epsilon\pi\beta} C_+}{2i(\sqrt{2r_c} \sin 2\theta)^\beta \sin\pi\beta} \sqrt{\frac{r_c}{2}}, \tag{35c}$$

$$E_- = \epsilon \frac{C_+ - e^{i\epsilon\pi\beta} C_-}{2i(\sqrt{2r_c} \sin 2\theta)^\beta \sin\pi\beta} \sqrt{\frac{r_c}{2}}, \tag{35d}$$

$$E_o = \frac{e^{i\epsilon\pi\beta/2} C_- - e^{-i\epsilon\pi\beta/2} C_+}{2(\sqrt{2r_c} \sin 2\theta)^\beta \sin\pi\beta} \sqrt{\frac{r_c}{2}}. \tag{35e}$$

It depends only on the angle θ, the radius of curvature of the boundary at the critical point, and the behavior of $U_{0n}(\mathbf{x}_S)$ close to the critical point via the coefficients C_+, C_-, and the singularity exponent β.

When β is an integer, the above analysis breaks down. However, the special case $\beta = 0$ has a solution. In that case, since (21a) and (21b) still apply, one can expect a singularity of G' in $(-x_\perp^{\rm NW})^{-1/2}$ but F' should remain regular and simply given by a constant $F'(0)$. This means that we should still have (26), (27a), (27b), and (28) with (30) and (31a) and (31b) for $\beta = 0$. Equations (33a) and (33b) obtained for $\beta = 0$ are then still valid. They admit a solution only if $C_+ = C_- = U_{0n}(0)$. This solution is

$$E_+ = (U_{0n}(0) + \sin 2\theta F'(0))\sqrt{\frac{r_c}{2}}, \tag{36a}$$

$$E_- = -E_+, \tag{36b}$$

$$E_o = i\epsilon E_+, \tag{36c}$$

$$D_+ = D_- = F'(0). \tag{36d}$$

It depends on an undetermined constant $F'(0)$ which is the opposite of the velocity of the wave packet emitted in the direction $\mathbf{e}_\parallel^{\rm NE}$ on the critical ray [see expression (11)].

III. VISCOUS SMOOTHING OF THE CRITICAL SLOPE SINGULARITY

In a real fluid, diffusion or viscosity is expected to smooth inviscid singularities. Critical slope singularities can be smoothed as well.

We have seen that the singular inviscid solution that propagates in the north-west direction can be written (for $x_\perp^{\rm NE} > 0$) as

$$u_\parallel^{\rm NW} \underset{x_\perp^{\rm NW}\to 0}{\sim} \begin{cases} \dfrac{E_o}{(x_\perp^{\rm NW})^\mu} & \text{for } x_\perp^{\rm NW} > 0, \\ \dfrac{E_o e^{-i\epsilon\pi\mu}}{(-x_\perp^{\rm NW})^\mu} & \text{for } x_\perp^{\rm NW} < 0. \end{cases} \tag{37}$$

The viscous smoothing of a singularity of this form has already been studied by Moore and Saffman [14] for rotating fluids and Thomas and Stevenson [17] for stratified fluids. An expression valid for a general rotating and stratified fluid has been given in Le Dizès [22]. For a 2D configuration without buoyancy diffusion (infinite Prandtl number), this expression is

$$u_\parallel^{\rm NW} \sim C^{\rm NW} H_\mu(\zeta^{\rm NW}, x_\parallel^{\rm NW}) = C^{\rm NW} \frac{h_\mu(\zeta^{\rm NW})}{(x_\parallel^{\rm NW})^{\mu/3}}, \tag{38}$$

where $\zeta^{\rm NW}$ is the self-similar variable

$$\zeta^{\rm NW} = \epsilon \frac{x_\perp^{\rm NW}}{(x_\parallel^{\rm NW}\Lambda\nu/\omega)^{1/3}}, \tag{39}$$

with

$$\Lambda = \frac{2\gamma^2\cos^2\theta + \sin^2\theta}{\sin 2\theta|\gamma^2 - 1|}, \quad \gamma = 2\Omega/N, \tag{40}$$

and $h_\mu(\zeta)$ is the Moore-Saffman Thomas-Stevenson function

$$h_\mu(\zeta) = \frac{e^{-i\mu\pi/2}}{(\mu-1)!}\int_0^{+\infty} e^{ip\zeta - p^3} p^{\mu-1} dp, \tag{41}$$

defined for $\mu > 0$. The function $h_\mu(\zeta)$ satisfies [14]

$$h_\mu(\zeta) \sim \frac{1}{|\zeta|^\mu} \quad \text{as } \zeta \to +\infty, \tag{42a}$$

$$h_\mu(\zeta) \sim \frac{e^{-i\mu\pi}}{|\zeta|^\mu} \quad \text{as } \zeta \to -\infty. \tag{42b}$$

A simple matching of (38) with (37) then gives

$$C^{\mathrm{NW}} = \left(\frac{\omega}{\nu\Lambda}\right)^{\mu/3} e^{i\frac{\pi}{2}\mu(1-\epsilon)} E_o. \tag{43}$$

The expression (38) with (39) and (43) describes a localized beam of width $(x_\parallel^{\mathrm{NW}}\Lambda\nu/\omega)^{1/3}$ and velocity amplitude $[\omega/(\nu\Lambda x_\parallel^{\mathrm{NW}})]^{\mu/3}E_o$. Note in particular that the beam becomes wider and weaker as we get away from the critical point.

A similar analysis can be done for the beam propagating in the south-east direction. If we define $\mathbf{e}_\parallel^{\mathrm{SE}} = -\mathbf{e}_\parallel^{\mathrm{NW}}$ and $\mathbf{e}_\perp^{\mathrm{SE}} = -\mathbf{e}_\perp^{\mathrm{NW}}$, then the inviscid solution propagating in the SE direction that agrees with (37) is

$$u_\parallel^{\mathrm{SE}} \underset{x_\perp^{\mathrm{SE}}\to 0}{\sim} \begin{cases} \dfrac{-E_o e^{i\epsilon\pi\mu}}{(x_\perp^{\mathrm{SE}})^\mu} & \text{for } x_\perp^{\mathrm{SE}} > 0, \\ \dfrac{-E_o}{(-x_\perp^{\mathrm{SE}})^\mu} & \text{for } x_\perp^{\mathrm{SE}} < 0. \end{cases} \tag{44}$$

We then immediately obtain

$$u_\parallel^{\mathrm{SE}} \sim C^{\mathrm{SE}} H_\mu(\zeta^{\mathrm{SE}}, x_\parallel^{\mathrm{SE}}), \tag{45}$$

with $C^{\mathrm{SE}} = -e^{i\epsilon\mu\pi}C^{\mathrm{NW}}$.

It is worth mentioning that the above analysis is valid only if the nonviscous approximation (37) applies when $|x_\perp| \gg (x_\parallel\Lambda\nu/\omega)^{1/3}$ close to the critical point. This property is satisfied for the beams propagating in the NW and SE directions because the width of the viscous boundary layer remains of order $\nu^{2/5}$ [which corresponds to $x_\perp^{\mathrm{NW}} = O(\nu^{2/5})$] at a distance $x_\parallel^{\mathrm{NW}} = O(\nu^{1/5})$ from the critical point [12,23,24].

By contrast, for the beam propagating in the NE direction, viscous effects are expected to appear close to the critical point as soon as $x_\perp^{\mathrm{NE}} = O(\nu^{1/5})$. The beam propagating in that direction is possibly larger and not described by the similarity solution.

IV. CRITICAL SLOPE SINGULARITIES GENERATED BY NORMAL AND TANGENTIAL DISPLACEMENTS

A. Normal displacement

This situation corresponds to a generic configuration where the object is displaced in translation or subject to an external oscillating flow. In the linear regime, these two configurations are equivalent. What is important is the normal velocity of the object boundary close to the critical point with respect to the fluid. When there is a normal displacement, this velocity is nonzero and given by the projection of the boundary velocity along the normal vector at the critical point,

$$U_{0n}\big(\mathbf{x}_{\mathcal{S}_c}\big) = \mathbf{U}_0 \cdot \mathbf{n}\big(\mathbf{x}_{\mathcal{S}_c}\big) = U_{0x}\sin\theta + U_{0z}\cos\theta, \tag{46}$$

if $\mathbf{U}_0 = (U_{0x}, U_{0z})$ is the velocity in the (x, z) plane of the object boundary with respect to the fluid. The normal velocity is therefore not singular and given by expression (25) with $\beta = 0$ and $C_+ = C_- = U_{0n}(\mathbf{x}_{\mathcal{S}_c})$.

The nature of the singularity along the critical line is therefore expected to be always of the same nature with a velocity diverging as $(x_\perp^{\mathrm{NW}})^{-1/2}$. However, its amplitude cannot be obtained in closed

form. It depends on the velocity along the line $x_\perp^{\rm NE}=0$ from the critical point, that is, the constant $F'(0)$. As shown above, the velocity close to the critical line $x_\perp^{\rm NW}=0$ is given by

$$\mathbf{u}\sim G'(x_\perp^{\rm NW})\mathbf{e}_\parallel^{\rm NW}, \tag{47}$$

where

$$G'(x_\perp^{\rm NW})\underset{x_\perp^{\rm NW}\to 0}{\sim}\begin{cases}E_+(-x_\perp^{\rm NW})^{-1/2} & \text{for } x_\perp^{\rm NW}<0;\quad x_\perp^{\rm NE}>0\\ -E_+(-x_\perp^{\rm NW})^{-1/2} & \text{for } x_\perp^{\rm NW}<0;\quad x_\perp^{\rm NE}<0,\\ i\epsilon E_+(x_\perp^{\rm NW})^{1/2} & \text{for } x_\perp^{\rm NW}>0\end{cases} \tag{48}$$

with

$$E_+=[U_{0x}\sin\theta+U_{0z}\cos\theta+\sin 2\theta F'(0)]\sqrt{r_c/2}. \tag{49}$$

As an illustration, one can look at the flow generated by an oscillating circular cylinder in a nonrotating fluid. The general solution has been provided by Hurley [5] for an elliptic cylinder. For a circular cylinder of radius r_c, the solution is

$$\mathbf{u}(\sigma_+,\sigma_-)=u_+(\sigma_+)\mathbf{e}_\parallel^{\rm NE}+u_-(\sigma_-)\mathbf{e}_\parallel^{\rm NW}, \tag{50}$$

with

$$u_\pm(\sigma_\pm)=\alpha_\pm\left(1-\frac{\sigma_\pm}{\sqrt{\sigma_\pm^2-r_c^2}}\right), \tag{51}$$

where the constants $\alpha_\pm$ are given by

$$\alpha_\pm=\tfrac{1}{2}(iU_{0z}\pm U_{0x})e^{-i\theta}, \tag{52}$$

and the coordinates $\sigma_\pm$ are related to our coordinates $x_\perp^{\rm NE}$ and $x_\perp^{\rm NW}$ by

$$\sigma_+=-x_\perp^{\rm NE}-r_c\cos(2\theta), \tag{53}$$

$$\sigma_-=x_\perp^{\rm NW}+r_c. \tag{54}$$

The definition of the square root depends on the position with respect to the critical lines $\sigma_+=\pm r_c$ and $\sigma_-=\pm r_c$. Close to the critical point $(x_\perp^{\rm NE},x_\perp^{\rm NW})=(0,0)$, we get

$$u_+(\sigma_+)\sim\alpha_+[1-i\cot(2\theta)]=\frac{(U_{0z}-iU_{0x})e^{i\theta}}{2\sin 2\theta}=-F'(0), \tag{55}$$

and

$$u_-(\sigma_-)\sim\begin{cases}-i\sqrt{\frac{r_c}{2}}\alpha_-(-x_\perp^{\rm NW})^{-1/2} & \text{for } x_\perp^{\rm NW}<0,\quad x_\perp^{\rm NE}>0\\ i\sqrt{\frac{r_c}{2}}\alpha_-(-x_\perp^{\rm NW})^{-1/2} & \text{for } x_\perp^{\rm NW}<0,\quad x_\perp^{\rm NE}<0,\\ -\sqrt{\frac{r_c}{2}}\alpha_-(x_\perp^{\rm NW})^{-1/2} & \text{for } x_\perp^{\rm NW}>0\end{cases} \tag{56}$$

which is in agreement with formula (48) for the nonrotating case ($\epsilon=-1$) if one uses (55) for $F'(0)$ in E_+ and (52) for α_-.

As explained above, from the inviscid solution close to the singularity, one can immediately get the viscous solution smoothing the singularity. Along the NW and SE directions, this gives

$$u_\parallel^{\rm NW}\sim e^{i\frac{\pi}{4}(1+\epsilon)}E_+\left(\frac{\omega}{\nu\Lambda}\right)^{1/6}H_{1/2}(\zeta^{\rm NW},x_\parallel^{\rm NW}), \tag{57a}$$

$$u_\parallel^{\rm SE}\sim e^{i\frac{\pi}{4}(1-\epsilon)}E_+\left(\frac{\omega}{\nu\Lambda}\right)^{1/6}H_{1/2}(\zeta^{\rm SE},x_\parallel^{\rm SE}), \tag{57b}$$

where the function H_μ has been defined in (38)–(41), and E_+ is given by (49). These expressions show that the velocity field generated by a normal displacement is $O(\nu^{-1/6})$ larger near the critical line than the forcing amplitude. The amplitude nevertheless decreases as $x_\parallel^{-1/6}$ with the distance $x_\parallel$ from the critical point.

B. Tangential displacement

When the surface displacement is tangent to the surface, there is no inviscid forcing. The forcing of the wave is due in that case to the Ekman pumping generated by viscous effects close to the boundary. The Ekman pumping corresponds to the normal velocity u_n^{EP} that is generated outside the boundary layer by the viscous boundary layer solution. This quantity has been calculated in Appendix for a general tangential displacement $U_{0t}\mathbf{t} + U_{0y}\mathbf{e}_y$ of the boundary. It is given by (A19). This normal velocity provides the forcing term $U_{0n}(\mathbf{x}_S) = u_n^{\mathrm{EP}}$ of the waves.

Close to a critical point, the Ekman pumping exhibits a singular behavior which can be written in terms of the variable $x_\perp^{\mathrm{NE}}$ as

$$x_\perp^{\mathrm{NE}} \underset{s\to s_c}{\sim} -\sin 2\theta \alpha_c (s - s_c) \tag{58}$$

and

$$u_n^{\mathrm{EP}} \underset{x_\perp^{\mathrm{NE}}\to 0}{\sim} \mp\sqrt{\frac{\nu r_c}{\omega}} \frac{e^{\mp\epsilon i\pi/4}(\sin 2\theta)^{3/2}}{|x_\perp^{\mathrm{NE}}|^{3/2}} [\bar{F}_t(\theta, 2\Omega/N)U_{0t} + i\bar{F}_y(\theta, 2\Omega/N)U_{0y}], \tag{59}$$

where

$$\bar{F}_t(\theta,\gamma) = \frac{\gamma^2\cos^2\theta + \sin^2\theta}{2[\sin 2\theta(2\gamma^2\cos^2\theta + \sin^2\theta)|\gamma^2 - 1|]^{1/2}}, \tag{60a}$$

$$\bar{F}_y(\theta,\gamma) = \frac{\gamma\cos\theta}{2}\left[\frac{\gamma^2\cos^2\theta + \sin^2\theta}{\sin 2\theta(2\gamma^2\cos^2\theta + \sin^2\theta)|\gamma^2 - 1|}\right]^{1/2}. \tag{60b}$$

The normal velocity is therefore of the form (25) with $\beta = 3/2$ and

$$C^+ = e^{i\epsilon\pi/2}C^- = -e^{-i\epsilon\pi/4}\sqrt{\frac{\nu r_c}{\omega}}(\sin 2\theta)^{3/2}(\bar{F}_t U_{0t} + i\bar{F}_y U_{0y}). \tag{61}$$

Applying formulas (35a)–(35e) gives

$$D_+ = D_- = 0, \tag{62a}$$

$$E_o = -e^{i\epsilon\pi/4}E_+ = -e^{-i\epsilon\pi/2}E_- = \sqrt{\frac{\nu}{\omega}}\frac{r_c^{1/4}}{2^{5/4}}(\bar{F}_t U_{0t} + i\bar{F}_y U_{0y}). \tag{62b}$$

A tangential displacement of the boundary then gives rise to a critical slope singularity in $|x_\perp^{\mathrm{NW}}|^{-5/4}$ with an amplitude of order $\nu^{1/2}$.

As explained above, such a singularity, when smoothed by viscous effect produces a thin internal shear layer that can be described by the Moore-Saffman Thomas-Stevenson self-similar solution. The north-west and south-east critical slope beams are then given by

$$u_\parallel^{\mathrm{NW}} \sim C_0^{\mathrm{NW}} H_{5/4}(\zeta^{\mathrm{NW}}, x_\parallel^{\mathrm{NW}}), \tag{63a}$$

$$u_\parallel^{\mathrm{SE}} \sim C_0^{\mathrm{SE}} H_{5/4}(\zeta^{\mathrm{SE}}, x_\parallel^{\mathrm{SE}}), \tag{63b}$$

with

$$C_0^{\mathrm{NW}} = e^{i\frac{5\pi}{8}(1-\epsilon)}\left(\frac{\nu}{\omega}\right)^{1/12}\left(\frac{r_c}{2}\right)^{1/4}(\bar{G}_t U_{0t} + i\bar{G}_y U_{0y}), \tag{64a}$$

$$C_0^{\mathrm{SE}} = e^{i\epsilon\pi/4}C_0^{\mathrm{NW}}, \tag{64b}$$

and

$$\bar{G}_t = \frac{\bar{F}_t}{2\Lambda^{5/12}} = \frac{(\gamma^2\cos^2\theta + \sin^2\theta)}{4(\sin 2\theta)^{1/12}|\gamma^2-1|^{1/12}(2\gamma^2\cos^2\theta+\sin^2\theta)^{11/12}}, \tag{65a}$$

$$\bar{G}_y = \frac{\bar{F}_y}{2\Lambda^{5/12}} = \frac{\gamma\cos\theta(\gamma^2\cos^2\theta + \sin^2\theta)^{1/2}}{4(\sin 2\theta)^{1/12}|\gamma^2-1|^{1/12}(2\gamma^2\cos^2\theta+\sin^2\theta)^{11/12}}, \tag{65b}$$

where $\gamma = 2\Omega/N$ and H_μ has been defined in (38)–(41).

Expressions (63a) and (63b) with (64a) and (64b) mean that the localized beam on the critical line has a velocity amplitude scaling as $[\nu r_c^3/(\omega x_\parallel^5)]^{1/12}$ where $x_\parallel$ is the distance from the critical point.

Without stratification, we recover the expression obtained for a librating sphere [13,25,26] (note that He *et al.* [25] corrected a sign error in the expressions first given in Le Dizès and Le Bars [13]). This is not surprising as this expression was obtained by matching directly the boundary layer solution to the self-similar solution around the critical line. It was then implicitly assumed in Ref. [13] that nothing was emitted in the NE direction close to the critical point. The present analysis which gives $D_+ = D_- = 0$ permits one to justify this hypothesis.

V. HIGHER-ORDER CORRECTIONS TO THE CRITICAL SLOPE SINGULARITY

We have discussed above how an inviscid singularity is generically formed from a critical slope and how this singularity is possibly smoothed by viscosity.

We have seen that the mechanism of generation is essentially inviscid as the singularity properties (index and amplitude) are directly related to the velocity component normal to the boundary. The amplitude of the inviscid waves that are generated is such that their normal velocity matches the normal velocity of the boundary. These waves also possess velocity components that are tangential to the boundary. This tangential velocity is in principle cancelled in a viscous boundary layer. But this process also generates, via Ekman pumping, a normal velocity correction that is responsible of a correction to the emitted inviscid waves. It is the expression of this higher-order viscous correction that we want to calculate in this section.

The singular inviscid beam propagating in the north-west direction that is created from the critical point has a velocity component along $\mathbf{e}_\parallel^{\mathrm{NW}}$ given by an expression of the form (37). The corresponding transverse velocity u_y is given by (5). This gives a velocity tangent to the boundary surface $\mathcal{S}$ near the critical point which can be expressed as $\mathbf{u}_T = u_t\mathbf{t} + u_y\mathbf{e}_y$ with

$$u_t(\mathbf{x}_\mathcal{S}) \sim -u_\parallel^{\mathrm{NW}}(\mathbf{x}_\mathcal{S}), \tag{66a}$$

$$u_y(\mathbf{x}_\mathcal{S}) \sim \frac{2i\Omega\cos\theta}{\omega}u_\parallel^{\mathrm{NW}}(\mathbf{x}_\mathcal{S}). \tag{66b}$$

This tangential velocity has to be canceled in a boundary layer by adding a boundary layer solution satisfying the boundary conditions $u_t^{(0)}(0) = -u_t(\mathbf{x}_\mathcal{S})$ and $u_y^{(0)}(0) = -u_y(\mathbf{x}_\mathcal{S})$.

Such a solution has been calculated in Appendix. It is given by (A8) with (A10a), (A10b), and (A13) for the coefficients. It leads to an expression for the Ekman pumping given by (A14) and (A15). Close to the critical point, expression (A18) for $\tilde{u}_-$ reduces to

$$\tilde{u}_- \sim u_\parallel^{\mathrm{NW}}(\mathbf{x}_\mathcal{S}). \tag{67}$$

As both $\tilde{u}_-$ and λ_- are singular, the last two terms of (A15) now contribute to Ekman pumping. We obtain, in terms of the coordinate $x_\perp^{\rm NE}$,

$$u_n^{\rm EP} \underset{x_\perp^{\rm NE}\to 0}{\sim} \begin{cases} \dfrac{-C^{(v)}e^{-i\epsilon\pi(\mu+1/4)}}{|x_\perp^{\rm NE}|^{2\mu+3/2}} & \text{for } x_\perp^{\rm NE} > 0, \\ \dfrac{C^{(v)}e^{i\epsilon\pi(\mu+1/4)}}{|x_\perp^{\rm NE}|^{2\mu+3/2}} & \text{for } x_\perp^{\rm NE} < 0, \end{cases} \tag{68}$$

with

$$C^{(v)} = E_o\sqrt{\frac{\nu\Lambda}{\omega}}(\mu+1/4)\left(\frac{2}{r_c}\right)^{1/4}(\sqrt{2r_c}\sin 2\theta)^{2\mu+3/2}, \tag{69}$$

where Λ has been defined in (40).

If we apply the formula (35a)–(35e) with

$$C_+ = -C^{(v)}e^{-i\epsilon\pi(\mu+1/4)}, \tag{70a}$$

$$C_- = C^{(v)}e^{i\epsilon\pi(\mu+1/4)}, \tag{70b}$$

and $\beta = 2\mu + 3/2$, then we get

$$D_+^{(v)} = D_-^{(v)} = 0, \tag{71}$$

and

$$E_o^{(v)} = E_o\sqrt{\frac{\nu\Lambda}{\omega}}\left(\frac{r_c}{2}\right)^{1/4}(\mu+1/4), \tag{72a}$$

$$E_+^{(v)} = -e^{-i\epsilon\pi(\mu+1/4)}E_o^{(v)}, \tag{72b}$$

$$E_-^{(v)} = -e^{i\epsilon\pi(\mu+1/4)}E_o^{(v)}. \tag{72c}$$

This means that the viscous correction associated the critical slope singularity in $|x_\perp^{\rm NW}|^{-\mu}$ gives rise to a stronger singularity in $|x_\perp^{\rm NW}|^{-(\mu+5/4)}$. However, the amplitude has decreased by a factor proportional to $\sqrt{\nu/\omega}$. In the north-west direction, it then gives a viscous self-similar correction of the form

$$u_\parallel^{{\rm NW}(v)} \sim C^{{\rm NW}(v)}H_{\mu+5/4}(\zeta^{\rm NW}, x_\parallel^{\rm NW}), \tag{73}$$

with

$$C^{{\rm NW}(v)} = e^{i\frac{\pi}{2}(\mu+\frac{5}{4})(1-\epsilon)}\left(\frac{\omega}{\nu\Lambda}\right)^{\mu/3+5/12}E_o^{(v)}, \tag{74}$$

which can be written, using (43) and (72a), as

$$C^{{\rm NW}(v)} = C^{\rm NW}e^{i\frac{5\pi}{8}(1-\epsilon)}\left(\frac{\nu\Lambda}{\omega}\right)^{1/12}\left(\frac{r_c}{2}\right)^{1/4}(\mu+1/4). \tag{75}$$

Similarly, in the SE direction, we get

$$u_\parallel^{{\rm SE}(v)} \sim C^{{\rm SE}(v)}H_{\mu+5/4}(\zeta^{\rm SE}, x_\parallel^{\rm SE}), \tag{76}$$

with $C^{{\rm SE}(v)} = e^{i\epsilon\pi(\mu+1/4)}C^{{\rm NW}(v)}$.

In both NW and SE directions, the viscous correction is therefore smaller by a nondimensional factor of order $[\nu r_c^3/(\omega x_\parallel^5)]^{1/12}$ compared to the leading-order beam. Interestingly, no viscous correction is generated in the north-east direction.

VI. DISCUSSION

In this paper, we have analyzed the generic properties of the singularity generated by critical slopes on waves in a stratified and rotating unbounded fluid. We have shown that this singularity is of inviscid nature and results from a geometric focusing of the normal velocity forcing on the characteristic line tangent to the boundary. By applying the inviscid boundary conditions on the normal velocity close to the critical point and outwards boundary conditions at infinity, we have been able to obtain relations between coefficients on either side of the singularity lines. Two generic configurations have been considered: an oscillating translation leading to direct normal velocity forcing and a tangential boundary oscillation for which the normal velocity forcing results from Ekman pumping. For the first case, we have seen that the velocity singularity is in $|x_\perp|^{-1/2}$ but its amplitude cannot be obtained in closed form. For the second case, the velocity singularity is in $|x_\perp|^{-5/4}$ and an explicit expression for the amplitude is derived. This stronger singular behavior for the tangential forcing comes from the singular behavior of the Ekman pumping close to the critical point.

We have shown how the inviscid singularity can be smoothed by viscosity using the self-similar expression introduced by Moore and Saffman [14] and Thomas and Stevenson [17]. It leads to a thin shear layer of width of order $(\nu x_\parallel/\omega)^{1/3}$ and to a velocity amplitude in $[\omega r_c^3/(\nu x_\parallel)]^{1/6}$ for the first case and in $[\nu r_c^3/(\omega x_\parallel^5)]^{1/12}$ for the second case.

A viscous correction in $\nu^{1/12}$ generated by corrections in the viscous boundary layer has also been calculated for each case. This correction is larger than the next-order correction to the self-similar solution which is in $\nu^{1/3}$ [14] and also larger than the viscous correction in $\nu^{1/6}$ obtained when such a solution reflects on a fixed boundary [22].

The analysis has neglected buoyancy diffusivity. It is not an issue to add this effect in the smoothing of the critical slope singularity. The form of the self-similar Moore-Saffman Thomas-Stevenson solution in a rotating and stratified fluid when both viscosity and buoyancy diffusivity are present has been given in Ref. [22]. The same expression can be used here. Including buoyancy diffusivity in the boundary layer analysis is also possible. It leads to a sixth-order problem which can also be solved without difficulty if for instance the boundary condition on the buoyancy perturbation is $b(\mathbf{x}_S) = 0$. Another expression for the Ekman pumping is obtained but the analysis should be qualitatively similar if the background stratification is not modified close to the boundary. This is actually the issue if buoyancy diffusivity is present. The isopycnals are not expected to remain horizontal close to an inclined boundary. None of the classical boundary conditions $b_0(\mathbf{x}_S) = 0$ (isothermal) and $\nabla b_0(\mathbf{x}_S) \cdot \mathbf{n} = 0$ (no flux) is indeed compatible with our background stratification (horizontal isopycnals) close to the critical point. So in principle one should either add the transitory flow created in the boundary layer by the mismatch between the background stratification and the boundary condition [27] or modify the background stratification close to the boundary so that it is in agreement with the boundary condition of the problem. In both cases, the extension is then not trivial.

The analysis has focused on 2D unbounded geometries. The extension to 3D axisymmetric geometry should not be a problem. In that case, there is no global expression for the velocity, but as long as we are far from the vortex axis, curvature effects are negligible for singular behaviors. Moreover, a self-similar expression describing viscous smoothing also exists in axisymmetric geometries far from the axis (see Ref. [26], for instance). The analysis that has been done for a librating axisymmetric object in a rotating fluid in Le Dizès and Le Bars [13] can then be extended to other types of forcing and to a stratified fluid without difficulty using the results of the present study.

The extension to a closed domain is by contrast a much more complicated issue. In a closed domain, characteristic lines emitted from the critical point may come back to the critical point after reflections on the domain boundary. The condition of outward waves can then not be used anymore, and the analysis *a priori* breaks down. Depending on the frequency and on the geometry, the characteristics may be periodic, space filling or may converge towards an attractor. Each case is expected to be different for a given forcing. Nevertheless, He *et al.* [25,26] have demonstrated that, in a spherical shell, the linear periodic solution obtained by librating the inner sphere can still be related in many situations to the critical slope singularity generated from the critical point as if the fluid was unbounded.

Finally, it is worth mentioning that other boundary singularities such as corners or discontinuities could probably be treated by the same approach. The singularity generated by a boundary discontinuity is in particular expected to be in $|x_\perp|^{-1}$. It should then give rise to internal shear layers with a velocity amplitude in $\nu^{-1/3}$. It would be interesting to provide a complete theory for this case, and extend the present analysis to all possible singular boundary features.

APPENDIX: EKMAN PUMPING

In this section, we discuss the Ekman pumping coming from tangential displacement of a surface. We provide a general expression for the Ekman pumping close to a critical point, that is a general expression for the normal velocity that is generated by the boundary layer flow outside the boundary layer.

We consider the situation illustrated in Fig. 2. The curve $\mathcal{S}$ in the (x, z) plane is parametrized by s, and at any point $\mathbf{x}_\mathcal{S}$ on $\mathcal{S}$, we define the tangent and normal vectors $\mathbf{t}$ and $\mathbf{n}$, as shown in Fig. 2. At the critical point at $s = s_c$, the tangent vector $\mathbf{t}$ is oriented along $-\mathbf{e}_\parallel^{\mathrm{NW}}$,

$$\mathbf{t}(s_c) = -\mathbf{e}_\parallel^{\mathrm{NW}} = \cos\theta \mathbf{e}_x - \sin\theta \mathbf{e}_z \,. \tag{A1}$$

We dimensionalize length and timescales using a characteristic length l and the forcing frequency ω. Defining the Ekman number as

$$E = \frac{\nu}{\omega l^2}, \tag{A2}$$

the governing equations are

$$-i\omega\mathbf{u} + 2\Omega\mathbf{e}_z \times \mathbf{u} = -\boldsymbol{\nabla} p + b\mathbf{e}_z + E\,\Delta\mathbf{u}, \tag{A3a}$$

$$-i\omega b + N^2\mathbf{u}\cdot\mathbf{e}_z = 0, \tag{A3b}$$

$$\boldsymbol{\nabla}\cdot\mathbf{u} = 0. \tag{A3c}$$

Defining the tangent and normal velocity components,

$$u_t = \frac{x'u + z'w}{\alpha}, \quad u_n = \frac{-z'u + x'w}{\alpha}, \quad \text{with} \quad \alpha = \sqrt{x'^2 + z'^2}, \tag{A4}$$

where the prime denotes differentiation with respect to s, and introducing the boundary layer scalings

$$(u_t, u_y, u_n, b, p) = \left(u_t^{(0)}(s,\eta), u_y^{(0)}(s,\eta), \sqrt{E}u_n^{(0)}(s,\eta), b^{(0)}(s,\eta), \sqrt{E}p^{(0)}(s,\eta)\right), \tag{A5}$$

with

$$\eta = \frac{x_n}{\sqrt{E}}, \tag{A6}$$

we get from (A3a)–(A3c) at leading order,

$$-i\omega u_t^{(0)} - 2\Omega\frac{x'}{\alpha}u_y^{(0)} = \frac{\partial^2 u_t^{(0)}}{\partial\eta^2} + \frac{z'}{\alpha}b^{(0)}, \tag{A7a}$$

$$-i\omega u_y^{(0)} + 2\Omega\frac{x'}{\alpha}u_t^{(0)} = \frac{\partial^2 u_y^{(0)}}{\partial\eta^2}, \tag{A7b}$$

$$2\Omega\frac{z'}{\alpha}u_y^{(0)} = -\frac{\partial p^{(0)}}{\partial\eta} + \frac{x'}{\alpha}b^{(0)}, \tag{A7c}$$

$$-i\omega b^{(0)} + N^2\frac{z'}{\alpha}u_t^{(0)} = 0, \tag{A7d}$$

$$\frac{1}{\alpha}\frac{\partial u_t^{(0)}}{\partial s} + \frac{\partial u_n^{(0)}}{\partial\eta} = 0. \tag{A7e}$$

Equations (A7a), (A7b), and (A7d) form a homogeneous system for the functions $u_t^{(0)}$, $u_y^{(0)}$, and $b^{(0)}$. The general solution can be expressed as a sum of four exponential functions. Only two of these functions are bounded as $\eta \to +\infty$, so we get

$$u_t^{(0)} = \tilde{u}_- e^{-\lambda_- \eta} + \tilde{u}_+ e^{-\lambda_+ \eta}, \tag{A8a}$$

$$u_y^{(0)} = \tilde{v}_- e^{-\lambda_- \eta} + \tilde{v}_+ e^{-\lambda_+ \eta}, \tag{A8b}$$

$$b^{(0)} = \tilde{b}_- e^{-\lambda_- \eta} + \tilde{b}_+ e^{-\lambda_+ \eta}, \tag{A8c}$$

where $\lambda_\pm$ are the solution of positive real part satisfying

$$\lambda_\pm^2 = -\frac{i}{\omega}\left[\omega^2 - \frac{N^2 z'^2}{2\alpha^2} \pm \frac{1}{2}\left(\frac{N^4 z'^4}{\alpha^4} + \frac{16\Omega^2 x'^2 \omega^2}{\alpha^2}\right)^{1/2}\right]. \tag{A9}$$

Moreover, the amplitudes $\tilde{u}_\pm$, $\tilde{v}_\pm$, and $\tilde{b}_\pm$ are related to each other by

$$(\lambda_\pm^2 + i\omega)\tilde{v}_\pm = \frac{2\Omega x'}{\alpha}\tilde{u}_\pm, \tag{A10a}$$

$$i\omega \tilde{b}_\pm = \frac{N^2 z'}{\alpha}\tilde{u}_\pm. \tag{A10b}$$

This general solution is not valid up to the critical point where one of the $\lambda_\pm$ vanishes. As shown by Roberts and Stewartson [24], the boundary layer becomes larger with a width of order $E^{2/5}$ when we get to a distance of order $E^{1/5}$ from the critical point, and a different ansatz should be used in that region. In the following, we then assume that we are at a distance from the critical point that is large compared to $E^{1/5}$.

We assume that the velocity at the boundary is tangential and given by

$$u_t(\mathbf{x}_S) = U_{0t}(s), \tag{A11a}$$

$$u_y(\mathbf{x}_S) = U_{0y}(s). \tag{A11b}$$

This gives two additional equations

$$\tilde{u}_- + \tilde{u}_+ = U_{0t}, \tag{A12a}$$

$$\tilde{v}_- + \tilde{v}_+ = U_{0y}. \tag{A12b}$$

They can be used together with (A10a) to obtain $\tilde{u}_\pm$

$$\tilde{u}_\pm = \frac{(\lambda_\pm^2 + i\omega)U_{0t} - (\lambda_\pm^2 + i\omega)(\lambda_\mp^2 + i\omega)U_{0y}\alpha/(2\Omega x')}{\lambda_\pm^2 - \lambda_\mp^2}, \tag{A13}$$

from which we can also deduce $\tilde{v}_\pm$ and $\tilde{b}_\pm$ using (A10a) and (A10b).

The Ekman pumping is related to the value $u_{n\infty}^{(0)}$ of $u_n^{(0)}$ as η goes to infinity. It is given in dimensional form by the expression

$$u_n^{\mathrm{EP}} = \omega l \sqrt{E} u_{n\infty}^{(0)}. \tag{A14}$$

The function $u_n^{(0)}$ is obtained from (A7e) using the expression of $u_t^{(0)}$ that we have just obtained and the condition $u_n^{(0)}(\eta = 0) = 0$. The calculation is straightforward and gives

$$u_{n\infty}^{(0)} = \lim_{\eta\to\infty} u_n^{(0)} = -\frac{\tilde{u}'_+}{\alpha\lambda_+} + \frac{\tilde{u}_+\lambda'_+}{\alpha\lambda_+^2} - \frac{\tilde{u}'_-}{\alpha\lambda_-} + \frac{\tilde{u}_-\lambda'_-}{\alpha\lambda_-^2}. \tag{A15}$$

In (A14), this gives the general expression of Ekman pumping from any surface. We are interested in the behavior close to a critical point. At such a point s_c,

$$x'(s_c) = x'_c = \alpha_c \cos\theta, \quad z'(s_c) = z'_c = -\alpha_c \sin\theta, \tag{A16}$$

and one of the two $\lambda_\pm$ vanishes. More precisely, as we get close to s_c

$$\lambda_+^2 \underset{s\to s_c}{\sim} \lambda_{+c}^2 = -i\frac{N^2\sin^2\theta + 8\Omega^2\cos^2\theta}{\omega} = -i\omega - i\frac{4\Omega^2\cos^2\theta}{\omega}, \tag{A17a}$$

$$\lambda_-^2 \underset{s\to s_c}{\sim} -i\frac{\sin 2\theta(4\Omega^2 - N^2)\omega}{\omega^2 + 4\Omega^2\cos^2\theta}\frac{\alpha_c(s-s_c)}{r_c}. \tag{A17b}$$

These behaviors show that $u_{n\infty}^{(0)}$ is dominated by the last term of (A15). Taking into account that (A13) for $\tilde{u}_-$ reduces close to s_c to

$$\tilde{u}_- \underset{s\to s_c}{\sim} -i\frac{\omega U_{0t} + i2\Omega\cos\theta U_{0y}}{\lambda_{+c}^2} = \frac{\omega^2 U_{0t} + i2\omega\Omega\cos\theta\, U_{0y}}{\omega^2 + 4\Omega^2\cos^2\theta}, \tag{A18}$$

we obtain from (A14) and (A15) an Ekman pumping that can be written close to the critical point as

$$u_n^{\mathrm{EP}} \underset{s\to s_c}{\sim} \sqrt{\frac{\nu r_c}{\omega}}\frac{\mp e^{\mp\epsilon i\pi/4}}{(\alpha_c|s-s_c|)^{3/2}}(\bar{F}_t U_{0t} + i\bar{F}_y U_{0y}), \tag{A19}$$

where $\bar{F}_t$ and $\bar{F}_y$ are functions of θ and $\gamma = 2\Omega/N$ only

$$\bar{F}_t(\theta,\gamma) = \frac{\gamma^2\cos^2\theta + \sin^2\theta}{2\left[\sin 2\theta(2\gamma^2\cos^2\theta + \sin^2\theta)|\gamma^2 - 1|\right]^{1/2}}, \tag{A20a}$$

$$\bar{F}_y(\theta,\gamma) = \frac{\gamma\cos\theta}{2}\left[\frac{\gamma^2\cos^2\theta + \sin^2\theta}{\sin 2\theta(2\gamma^2\cos^2\theta + \sin^2\theta)|\gamma^2 - 1|}\right]^{1/2}. \tag{A20b}$$

In (A19), the upper sign is taken if $(s - s_c) < 0$, the lower sign if $s - s_c > 0$. We recall that the parameter ϵ is equal to $+1$ if $2\Omega > N$, -1 otherwise.

For $\gamma = 0$ (that is $\Omega = 0$) and $\gamma = \infty$ (that is $N = 0$), we therefore have

$$\bar{F}_t(\theta,0) = \sqrt{\frac{\tan\theta}{8}}, \quad \bar{F}_y(\theta,0) = 0, \tag{A21a}$$

$$\bar{F}_t(\theta,\infty) = \bar{F}_y(\theta,\infty) = \frac{1}{4\sqrt{\tan\theta}}, \tag{A21b}$$

which gives for the Ekman pumping

$$u_n^{\mathrm{EP}}(\Omega = 0) \sim \sqrt{\frac{\nu r_c}{N}}\frac{\mp e^{\pm i\pi/4}}{(\alpha_c|s-s_c|)^{3/2}}\frac{U_{0t}}{2\sqrt{2}\sqrt{\cos\theta}}, \tag{A22a}$$

$$u_n^{\mathrm{EP}}(N = 0) \sim \sqrt{\frac{\nu r_c}{2\Omega}}\frac{\mp e^{\mp i\pi/4}}{(\alpha_c|s-s_c|)^{3/2}}\frac{U_{0t} + iU_{0y}}{4\sqrt{\sin\theta}}. \tag{A22b}$$

[1] P. G. Baines, The reflexion of internal/inertial waves from bumpy surfaces. Part 2. Split reflexion and diffraction, J. Fluid Mech. **49**, 113 (1971).

[2] H. P. Greenspan, *The Theory of Rotating Fluids* (Cambridge University Press, Cambridge, UK, 1968).

[3] D. E. Mowbray and B. S. H. Rarity, A theoretical and experimental investigation of the phase configuration of internal waves of small amplitude in a density stratified liquid, J. Fluid Mech. **28**, 1 (1967).

[4] J. C. Appleby and D. G. Crighton, Internal gravity waves generated by oscillations of a sphere, J. Fluid Mech. **183**, 439 (1987).

[5] D. G. Hurley, The generation of internal waves by vibrating elliptic cylinders. Part 1. Inviscid solution, J. Fluid Mech. **351**, 105 (1997).

[6] D. G. Hurley and G. Keady, The generation of internal waves by vibrating elliptic cylinders. Part 2. Approximate viscous solution, J. Fluid Mech. **351**, 119 (1997).
[7] B. Voisin, Near-field internal wave beams in two dimensions, J. Fluid Mech. **900**, A3 (2020).
[8] B. Voisin, Boundary integrals for oscillating bodies in stratified fluids, J. Fluid Mech. **927**, A3 (2021).
[9] H. P. Zhang, B. King, and H. L. Swinney, Experimental study of internal gravity waves generated by supercritical topography, Phys. Fluids **19**, 096602 (2007).
[10] F. Pétrélis, S. Llewellyn Smith, and W. R. Young, Tidal conversion at submarine ridge, J. Phys. Ocean. **36**, 1053 (2006).
[11] P. Echeverri and T. Peacock, Internal tide generation by arbitrary two-dimensional topography, J. Fluid Mech. **659**, 247 (2010).
[12] R. R. Kerswell, On the internal shear layers spawned by the critical regions in oscillatory Ekman boundary layers, J. Fluid Mech. **298**, 311 (1995).
[13] S. Le Dizès and M. Le Bars, Internal shear layers from librating objects, J. Fluid Mech. **826**, 653 (2017).
[14] D. W. Moore and P. G. Saffman, The structure of free vertical shear layers in a rotating fluid and the motion produced by a slowly rising body, Philos. Trans. R. Soc. A **264**, 597 (1969).
[15] I. C. Walton, Viscous shear layers in an oscillating rotating fluid, Proc. R. Soc. Lond. A **344**, 101 (1975).
[16] K. S. Peat, Internal and inertial waves in a viscous rotating stratified fluid, Appl. Sci. Res. **33**, 481 (1977).
[17] N. H. Thomas and T. N. Stevenson, A similarity solution for viscous internal waves, J. Fluid Mech. **54**, 495 (1972).
[18] N. Machicoane, P.-P. Cortet, B. Voisin, and F. Moisy, Influence of the multipole order of the source on the decay of an inertial wave beam in a rotating fluid, Phys. Fluids **27**, 066602 (2015).
[19] B. Voisin, Limit states of internal wave beams, J. Fluid Mech. **496**, 243 (2003).
[20] S. Le Dizès, Wave field and zonal flow of a librating disk, J. Fluid Mech. **782**, 178 (2015).
[21] P. G. Baines, The reflexion of internal/inertial waves from bumpy surfaces, J. Fluid Mech. **46**, 273 (1971).
[22] S. Le Dizès, Reflection of oscillating internal shear layers: Nonlinear corrections, J. Fluid Mech. **899**, A21 (2020).
[23] S. Kida, Steady flow in a rapidly rotating sphere with weak precession, J. Fluid Mech. **680**, 150 (2011).
[24] P. H. Roberts and K. Stewartson, On the stability of a MacLaurin spheroid of small viscosity, Astrophys. J. **137**, 777 (1963).
[25] J. He, B. Favier, M. Rieutord, and S. Le Dizès, Internal shear layers in librating spherical shells: The case of periodic characteristic paths, J. Fluid Mech. **939**, A3 (2022).
[26] J. He, B. Favier, M. Rieutord, and S. Le Dizès, Internal shear layers in librating spherical shells: The case of attractors, J. Fluid Mech. **974**, A3 (2023).
[27] C. Garrett, P. MacCready, and P. Rhines, Boundary mixing and arrested Ekman layers: Rotating stratified flow near a sloping boundary, Annu. Rev. Fluid Mech. **25**, 291 (1993).